BENEFITS AND CHALLENGES OF A MULTIFUNCTIONAL LEADING-EDGE SYSTEM FOR HIGH-EFFICIENCY TRANSPORT AIRCRAFT

O. Krawehl*, L.-H Lemke*, F. Thielecke*, M. Hillebrand †

* Hamburg University of Technology, Institute of Aircraft Systems Engineering, Nesspriel 5, D-21129 Hamburg, Germany
† University of Stuttgart, Institute of Aerodynamics and Gas Dynamics, Wankelstraße 3, D-70563 Stuttgart, Germany

Abstract

The improvement of aerodynamic performance is a key research aspect in the context of current and modern aircraft design. This is represented in multiple approaches addressing future aircraft optimization. The present study places a particular emphasis on the design of the wing and the corresponding flight control systems, such as high-aspect-ratio wings featuring laminar flow technologies and load alleviation systems. For the realisation of these approaches, it is necessary to rethink the functions of leading-edge devices and extend their capabilities from a simple high-lift system to a multifunctional control system. This design, enabling the proposed multifunctionality of high lift, load alleviation, and laminar flow, is yet to be developed, and it is therefore unclear whether the integration of such a system on the leading edge is feasible. Especially the resulting requirements and constraints regarding the actuation system of a multifunctional leading-edge control device pose significant challenges to the realisation of such a system. This paper aims to investigate the correlating and contradicting factors resulting from the combination of high-lift and load alleviation functionalities within one system. Furthermore, challenges regarding the system design are indicated.

Keywords

flight control system; high lift; load alleviation; laminar wing; actuation system; system design

1. INTRODUCTION

In recent studies, it was shown that laminar flow technologies can significantly improve aerodynamic aircraft performance by reducing drag [1] [2] [3]. While natural laminar flow (NLF) technologies have been designed successfully for low-swept-wing applications, especially in gliders [4] and general aviation aircraft [5], NLF wings are not a feasible solution for application to commercial transport aircraft at transonic speed.

Due to the cross-flow and attachment-line instabilities associated with transport aircraft wings, which are optimized to fly at higher Mach and Reynolds numbers, a more suitable option concerning laminar flow exists in the form of hybrid laminar flow control (HLFC) technologies. Improved laminar flow is achieved by the combination of optimized aerodynamic design and active or passive suction systems. A prominent example of this can be found in the tailplane section of the BOEING 787 Dreamliner [6]. The implementation of HLFC on the leading edge will have a substantial impact on the design of control surfaces and their actuation systems. Firstly, a typical HLFC profile is more slender with a reduced nose radius, which significantly complicates the integration effort. This challenge is further complicated by the additional system components of suction systems installed in the wing. Secondly, the leading edge must remain free of gaps to avoid turbulence wedges, which renders solutions including conventional leading-edge devices like slats infeasible. Lastly, secondary power provided by the engine generators is limited, therefore requiring sophisticated control and scheduling logic in order to manage power consumption.

A second area of interest promising performance gains can be found in the concepts of gust and manoeuvre load alleviation. Load alleviation can be achieved either by passive measures, such as aeroelastic tailoring, or by a dedicated system actively deflecting control surfaces to reduce the loads imposed on the wing. This approach is a promising enabler for performance gains because critical design loads are lower than those of a baseline wing without a load control system. This enables the application of higher aspect ratios, contributing to a reduction of lift-induced drag. In the past, active load control systems using trailing-edge devices [7] [8] or aileron deflection [9] for bending-moment reduction were proposed, while more recent studies also mention leading-edge flaps for the purpose of torsional-moment compensation and pitching-moment control [10] [11] [12] [13]. In this context, KRALL et al. [14] investigated potential system architectures and actuation technologies capable of providing load control capabilities. Their study of electromechanical actuation systems for leading-edge and trailing-edge devices concluded with the result of such a system introducing a substantial increase in system weight and power demand. Based on these findings and the results of the current work, the authors of this paper consider it plausible that, by separating the inboard leading-edge devices from the inboard devices using hydraulic actuators on the outboard section of the wing, a system providing a load alleviation function (LAF) using leading-edge devices is feasible. Furthermore, the same actuation system and control surfaces will be used to provide lift augmentation in low-speed flight, therefore necessitating a novel system design on the leading edge.

However, significant challenges arise when integrating multiple functionalities within a single actuation system. In particular, the constraints imposed by an HLFC wing design, system requirements, and resulting compromises at the overall aircraft level are of major concern. For this purpose, the key points to be addressed in the context of actuation system design for a multifunctional leading-edge system are discussed in this work. It is aimed at showing a possible system-technical solution while discussing its benefits and limitations.

2. REFERENCE AIRCRAFT WITH A NOVEL LEADING EDGE SYSTEM

An aircraft configuration, representative of a future high-efficiency long-range transport aircraft, is used for the investigations in this paper. This configuration is based on the aircraft that was developed by the German Aerospace Center (DLR) as part of the LuFo-project INTELWI and features high-aspect-ratio wings ($\Lambda = 12.38$) with a wingspan of $b = 62.18, \mathrm{m}$. A graphical representation of the aircraft with a highlighted leading edge is depicted in Figure 1.

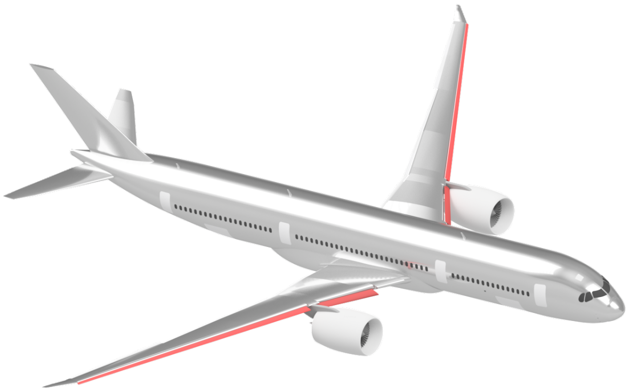

FIG 1. INTELWI reference aircraft configuration

The baseline INTELWI aircraft features a fully turbulent wing. For the improvement of the aircraft's aerodynamic performance, the wing shall be optimised toward prolonged laminar flow. Therefore, modification and redesign of the wing profile are mandatory to equip the aircraft with a low-drag, laminar wing. The goal of the modification is to delay the transition to turbulence on the outer part of the wing to 50 % of the wing chord on the upper and lower wing surfaces. This shall be achieved by using HLFC technology with an active suction system. In the context of actuation system design for a novel multifunctional leading edge, in-depth design of an HLFC system is not part of this work. Nevertheless, it is assumed to be a boundary condition that must be acknowledged for considerations regarding the actuation system. In particular, this affects the amount of available power for other system functions and the available installation space within the wing due to the space taken up by components of the suction system. These result from several factors, such as the suction panel itself as well as ducts and compressors that must be installed in the wing, as discussed by Iyer [15]. Furthermore, space limitations are imposed by the geometric conditions that are obtained from the HLFC wing profile design. Initial aerofoil optimisations conducted at the Institute of Fluid Mechanics of the Technische Universität Braunschweig resulted in a reduced nose radius as well as a thickness reduction at the front spar location. These factors impact the available installation space in the wing. In order to further improve the performance of the baseline aircraft, a novel leading-edge system is to be applied to the aircraft. The leading-edge system shall enable the functions of high lift, torsional load control, laminar flow, as well as protective functions such as ice protection of the wing.

In total, the wing of the reference aircraft is equipped with nine leading-edge control devices (LECDs), of which one is located between the fuselage and engine and eight are located outboard of the engine and are therefore called outboard LECDs. The trailing-edge devices are composed of an inboard flap, four multifunctional control devices (MFCDs), and four ailerons. A schematic view of the wing, indicating the control-surface layout, is provided in Figure 2. In this paper, only the actuation system of the leading-edge devices is discussed. However, it is important to recognise that the leading-edge and trailing-edge devices are working simultaneously to provide effective load alleviation with both torsion and bending-moment reduction. Additionally, the trailing-edge devices must also be actuated during the high-lift phase. Therefore, the trailing-edge control system limits the power budget that is available to the leading edge, and a failure in either one of those systems must not impede the functionality of the other system.

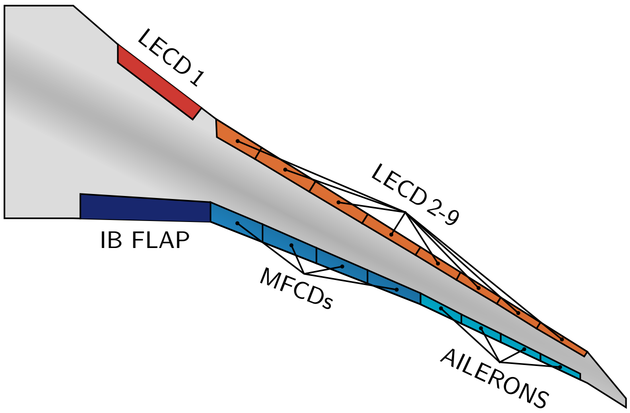

FIG 2. Schematic of control surface layout

The economical and ecological benefit of the multifunctional leading-edge system can primarily be measured in terms of the fuel consumption during a design mission. As the fuel consumption for two design missions is known from the INTELWI project, on which the reference aircraft is based, a direct comparison of the values is possible. This enables the formulation of a quantitative statement regarding the benefit of the multifunctional leading-edge system. The evaluation is based on the Breguet range equation

$$(1) \qquad R = E \cdot \frac{V}{b_\mathrm{f} \cdot g} \cdot \ln\left(\frac{m_\mathrm{ZWF}}{m_\mathrm{ZF} - m_\mathrm{fuel}}\right) \quad ,$$

which can be re-arranged to obtain the fuel mass m_fuel required for a given design mission

$$(2) \qquad m_\mathrm{fuel} = m_\mathrm{ZF} \cdot \left(e^{\frac{R \cdot b_\mathrm{f} \cot g}{V \cdot E}} - 1\right) \quad ,$$

with the zero-fuel mass m_ZF, the range R, the specific fuel consumption b_f, gravitational acceleration g, the aircraft's velocity V, and the glide ratio E. With the installation of a multifunctional leading-edge system, three main parameters of Equation 2 are affected. Firstly, the specific fuel consumption is expected to be above baseline due to the increased secondary power demand, especially from the load alleviation system and the active suction system installed in the wing. Secondly, the glide ratio will be impacted in two ways. With the possibility of load alleviation, higher-aspect-ratio wings can be designed in a cantilever configuration without the need for structural supports or reinforced wing structures. This offers the benefit of reducing lift-induced drag and thus improves the glide efficiency. Furthermore, the HLFC function of the system improves drag characteristics, as friction can be greatly reduced by delaying the transition to turbulence. Lastly, additional benefits can be achieved by reduction of the zero-fuel mass. This parameter depends on the trade-off between the reduction of structural mass versus the mass introduced by system components and associated attachments of both the HLFC and the load alleviation systems. A change of the zero-fuel mass is also likely to influence the fuel mass that must be carried for a flight mission, as snowball effects apply, which alter the fuel mass either positively or negatively. Therefore, a net reduction of zero-fuel mass, meaning the reduction of structural weight surpasses the added system mass, is desired, as this could potentially allow for a downsizing of engines, the fuel tank, as well as brakes, which could in turn further reduce the structural mass of the aircraft.

3. ACTUATION SYSTEM REQUIREMENTS

Requirements for the multifunctional leading-edge actuation system differ significantly from those of conventional leading-edge devices. A particular focus must be placed on the conflicting system requirements for the load alleviation and the high-lift function. The load alleviation function, active under cruise conditions, introduces an entirely new use case for leading-edge control devices, therefore necessitating a redesign of the actuation system. The solution space for the novel leading edge is restricted by internal and external constraints and requirements of the system. This includes loads, control-surface deflection angles and rates, as well as dependencies of the leading-edge system and other aircraft-level functions. Here, the HLFC function and environmental protections of the wing are regarded as boundary conditions. Additional requirements arise from safety-relevant aspects that must be considered for certification.

3.1. Loads and control surface deflection

According to Appendix K of the EASA CS-25 [16], structural safety factors may be reduced if the aircraft is equipped with a load alleviation system fulfilling its functions to a certain degree of reliability. To evaluate the load alleviation capabilities of the novel leading-edge system, a critical design load case is chosen, which simultaneously represents the dimensioning load case for the actuation system. The critical load case is a discrete $1-\cos$ gust encounter in cruise flight at $Ma = 0.83$ at an altitude of $z = 10,363$ m. The design gust is calculated according to CS-25.341 [16] for a gust gradient of $H = 50$ m and a gust velocity of $U = 13.2\,\frac{\text{m}}{\text{s}}$.
The resulting peak loads for each LECD were calculated at the Institute of Aerodynamics and Gas Dynamics of the University of Stuttgart and are summarized in Table 1. These are expressed as the hinge moment of the respective control surface. From these values, it is evident that the aerodynamic loads on the inboard wing range from double to ten times the hinge moments on the outboard wing. This indicates that it is more realistic to achieve a feasible solution in the outboard wing section.

	LE 1	LE 2	LE 3	LE 4	LE 5	LE 6	LE 7	LE 8	LE 9
M_h [kN·m]	20.90	9.95	10.15	7.70	5.75	3.36	2.75	2.22	1.90

TAB 1. Critical load case

The given loads refer to a wing root bending moment (WRBM) reduction of 33 %. A further reduction of bending moment may seem more beneficial at first glance; however, these benefits are limited to a mere improvement of passenger comfort. CS-25 Appendix K permits the safety factor to be reduced to the point where the structure is required to withstand two-thirds of the specified ultimate loads for the remaining flight with the load alleviation system in its failed state. Therefore, no additional savings in structural mass are achievable, as the structures must be designed to the same limit loads for load alleviation capabilities of more than 33 %. Furthermore, an extension of the load alleviation capabilities will lead to an increase of system mass, as actuators, kinematics, and fittings must be sized accordingly to the higher load, displacement, and deflection rate requirements resulting from a higher reduction of WRBM.
The aerodynamic loads acting on the LECDs depend on the gust penetration distance of the aircraft. Thus, a time-dependent load profile results from the gust encounter. In addition, this load profile varies depending on the span-wise location of the respective LECD. For the LECDs located closer to the fuselage, a profile corresponding with the $1-\cos$ shape of the discrete gust can be observed. Due to the flow separations occurring on the outboard section of the wing, the load profile differs significantly, which must be accounted for in the deflection of the control surfaces. A graphical representation of the characteristic load profiles on the wing without control-surface deflection in relation to the static load is provided in Figure 3.

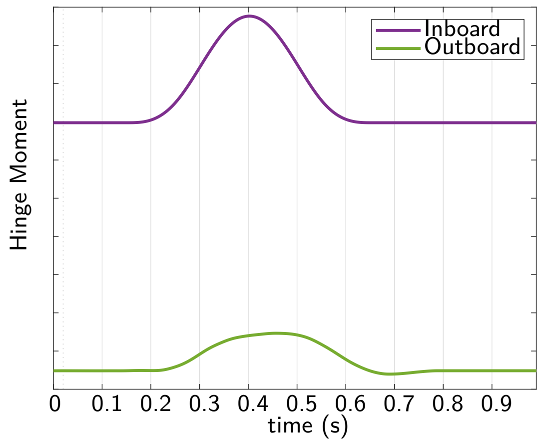

FIG 3. Characteristic load profile of a 1-cos gust encounter

While trailing-edge control devices must be deflected upwards to reduce WRBM, the leading-edge control devices must be deflected downwards in order to counteract the torsional moment as well as the pitching moment of the aircraft. The required maximum control-surface deflections and deflection rates for a load alleviation of 33 % of the critical design gust load are summarized in Table 2. For the redistribution during the gust encounter, only LECDs 2–9 are used, as preliminary calculations show that the use of LECD 1 could increase the torsional moment.

	LE 2	LE 3	LE 4	LE 5	LE 6	LE 7	LE 8	LE 9
δ [°]	4.5	5.8	5.6	6.0	7.0	6.6	6.1	6.0
$\dot{\delta}$ [°/s]	31.8	45.0	43.5	46.6	54.4	51.2	47.4	46.6

TAB 2. LECD deflection angles and rates

There is a significant difference between control-surface deflection during load alleviation and high-lift operation. High-lift functionality must be provided at two points in a typical mission: take-off and approach/landing. The actuation system of the leading edge is only actively deployed against loads during the approach phase. In general, the loads to overcome are significantly lower than those of the design gust. Therefore, the loads during high-lift operation are non-dimensioning for the actuation system. However, it must be acknowledged that the maximum deflection during high-lift is significantly greater than it is for load alleviation. The maximum high-lift deflection for the LECD is set to 27°, as depicted in [17] for the outboard leading-edge devices of an aircraft of similar size and use case. This position shall be assumed uniformly across the entire leading edge. Contrary to the load alleviation function, all LECDs (1–9) are used during high-lift. The deflection in this case is significantly slower. The LECDs shall be fully deployed after 20 seconds, which is comparable to the deployment time of high-lift devices in modern commercial transport aircraft. This yields an average deflection rate of $1.35^\circ/\mathrm{s}$. The maximum position as well as the deflection rate are arbitrarily chosen at this point. Further optimization of this might be conducted in later design steps if aerodynamic performance during high-lift can be maximized by a different high-lift position.

3.2. Power requirements

Secondary power, produced by the engine generators, is limited and must be allocated to the functions of the aircraft. This can be especially challenging in the context of multi-functionality, as the available power is a limiting factor and might prevent functions from working simultaneously. A first allocation of available power is conducted using cruise data of the BOEING 787 [18]. The available secondary power of the aircraft, approximately 1,000 kVA, is increased by 20 % to account for future engine and generator development. Therefore, 1,200 kVA of secondary power is taken as a realistic budget for the reference aircraft featuring the novel leading-edge system. In the 787 nominal cruise data, the power is divided between the flight control system (approx. 55 kVA), environmental control system (approx. 390 kVA), ice protection (approx. 60 kVA), galleys (approx. 120 kVA), and other systems such as cabin systems, lights, etc. (approx. 319 kVA). Taking this into account, there is a remaining headroom of approximately 260 kVA available for the functions of the multi-functional leading-edge system. A first estimate of the power required for an HLFC system is taken from [19], suggesting a budget of 250 kVA must be attributed to the wing suction system. Thus, there is no realistic amount of power available for the load alleviation function when the suction system is active at the same time. This issue can, however, be solved by shedding some of the non-essential power consumers during a gust encounter. The wing suction system is switched off during gust encounters, as laminarity will be lost regardless of the HLFC system. Therefore, operation with active HLFC does not provide benefits during gust load encounters. This is achieved by switching off the galleys and reducing the ice protection to a low-power-consumption mode. This allows for a realistic power allocation for the load alleviation function, prioritising the protection of the structure from overload. Therefore, two main operational modes result: nominal cruise with active HLFC and icing protection, as well as cruise with active load alleviation (LAF), with the respective power budgets. These are displayed in Figure 4. A rapid transition between these two regimes must be enabled, including the necessary means of protection from power fluctuations. The power budget of 400 kVA for the load alleviation function is consumed by both the leading-edge as well as the trailing-edge load alleviation system on both wings of the aircraft. Following the results of the investigations of trailing-edge LAF conducted during the INTELWI Project, a power budget of 90 kVA is allocated to the trailing-edge MFCDs and ailerons. This leaves a remaining maximum power budget of 310 kVA for the leading-edge actuation system in its load alleviation operation and is therefore a limiting sizing factor for the actuators and power supply system.

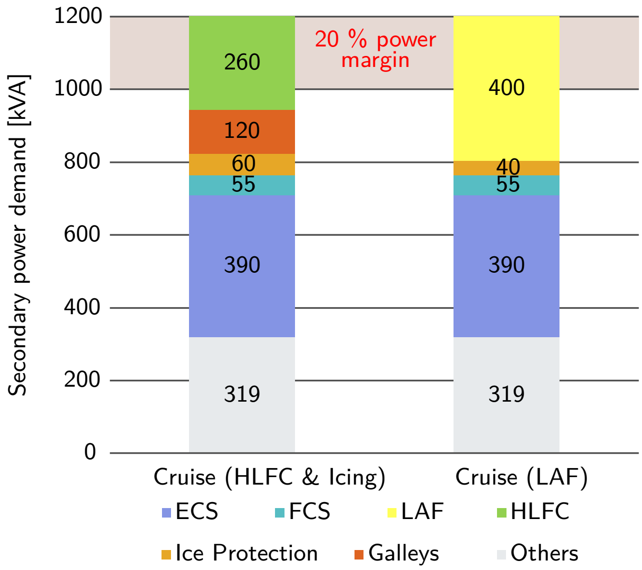

FIG 4. Secondary Power Consumption of AC functions

3.3. System safety and certification

Both the high-lift function as well as the load alleviation function are safety-critical flight control functions. Therefore, safety requirements according to certification standards are of utmost importance for the system design.
The assessment of potential certification requirements for the multifunctional leading-edge system is based on CS-25 [16] requirements for high-lift, flight control, and load alleviation systems. A central requirement is the reliability of the system. As stated in Appendix K of the CS-25, the safety factor for sizing of the aircraft structure may be reduced if the probability of failure occurrence for the load alleviation system can be shown to be below 10^{-5} failures per flight hour. This is achievable by several means, such as redundancy in the actuation system, supply systems, and load paths. Furthermore, safety components such as emergency brakes, commonly found in high-lift systems, can be included in the system architecture, preventing a catastrophic event from a single failure source, as dictated in §25.1309. Another viable solution lies within the segmentation of the leading edge itself. Preliminary investigation suggests enough load alleviation capability remains after a failure of up to three LECDs. However, it must be shown that a system failure of this gravity does not prevent continued safe flight of the aircraft (cf. §25.672).
Furthermore, it is stated in §25.671 that system failures, such as jamming and skewing, are assumed to occur in any flight phase and must also not impede safe handling of the aircraft. Therefore, adequate means for prevention of this failure, e.g. skew and asymmetry monitoring and mitigation, must be provided in the actuation system of the multifunctional leading-edge system. Furthermore, it is necessary to design system components, structures, etc., to be able to withstand the jam or skew loads, including those occurring in asymmetric flight conditions in any flight phase (cf. §§25.671, 25.701). Therefore, a limitation of deflection during cruise must be considered to avoid inadvertent extension of the LECDs to the high-lift position, which would exert high loads on the structures, risking a disconnection of the control surface.
As the same actuation system is used for both load alleviation and high-lift functionality, the requirements regarding system safety of the high-lift system must be fulfilled at the same time. A central requirement for high-lift systems is found in §25.701, stating that unless safe handling characteristics exist

for asymmetric deflection of HL devices on both sides of the aircraft, the symmetry must be synchronised by a mechanical interconnection or approved equivalent means. Due to the segmentation of the leading edge, in combination with the deflection angle and rate requirements, a mechanical interconnection between the control surfaces is unlikely to be a feasible solution for the system design. Therefore, the remaining solutions lie in either showing safe handling characteristics for the asymmetry failure case or providing equivalent means of synchronisation, which can be achieved by designing an actuation system with an integrated safety mechanism, limiting the range of deflection for each control surface.

4. TECHNOLOGY SELECTION

The combination of a load control function and HLFC technologies with a conventional leading-edge high-lift system is challenging in multiple ways. Dependencies of the individual functions and capabilities constrain the solution space for an overall system design. Key aspects include the selection of a control device, actuators, architecture topology, and safety features.

4.1. Selection of control device

Considering the individual functions, different device types are more suitable than others in the respective discipline. Three potential device types or combinations thereof were initially identified as solution candidates for a control surface. These include sealed slats, droop noses, and Krüger flaps, as displayed in Figure 5. As discussed by Krall et al. [20], raised Krüger flaps are a go-to solution for a high-lift device on a (natural) laminar wing, as they prevent contamination of the leading edge, which would cause turbulent flow. Evidently, Krüger flaps are a proven high-lift device concept, featured in multiple commercial transport aircraft [21]. However, these devices are not suitable for the purpose of load alleviation, as the rotational deflection from the underside of the wing is not effective in reducing torsional loads. Therefore, a solution featuring Krüger flaps requires combination with other device types to provide the multifunctionality discussed in this paper. This solution is considered unfavourable, as [20] already mentioned installation space conflicts even without additional HLFC system components incorporated in the wing. Therefore, the multifunctional leading edge must be realised using a different device type.

On modern commercial transport aircraft, slats can be viewed as a de facto standard for leading-edge control devices, used to provide high-lift capabilities in low-speed flight. In theory, slats could also be used for torsional load control, given they are designed in a sealed-slat configuration. Typically, slats open a slot between the slat body and fixed wing for stabilisation of the boundary layer. In a sealed-slat configuration, the slot is only open in the high-lift position and closed while the deflection is small. This feature is beneficial for effective torsional load alleviation. However, due to the fact that the slat and the wing are separate bodies, gaps and steps arise between the fixed wing and the slat, which in turn cause turbulence and significantly impede the effort to achieve laminar flow for 50 % of the wing chord. Therefore, the slat approach is also considered unfavourable. Nevertheless, a solution incorporating a gap-free device exists in the form of a droop nose device [22]. Specifically, the absence of gaps and steps applies to a morphing droop nose, meaning the control device is not a separate control surface but rather a section of the wing structure itself, which is flexible enough to allow variations of its shape. Nevertheless, sufficient rigidity must be provided in order to prevent deformation of the structure under air load. Therefore, the implementation of a droop nose exerts significant additional loads on the actuation system, due to the deformation work that must be generated by the actuators. As the droop nose does not create a slot, there is no stabilisation of the boundary layer on the upper wing surface. Therefore, the stall behaviour of droop nose devices is disadvantageous compared to the other high-lift devices. Nevertheless, sufficient high-lift performance remains in low-speed flight using this type of control device, especially when considering that less lift augmentation will be required for future high-efficiency wings. A secondary drawback associated with the droop nose is its inability to protect the leading edge against contamination. The authors are aware that a solution must be found to address the issue of turbulence resulting from leading-edge contamination. So far, consideration has been given to bug wipers, commonly found on gliders, piezo transducers for ultrasonic cleaning, as well as special wing surface coatings. However, this remains a topic for future investigations. Nevertheless, despite the mentioned disadvantages, the conceptual investigations regarding different LECD types showed a clear superiority of droop nose (DN) devices over other technologies for the intended multifunctionality.

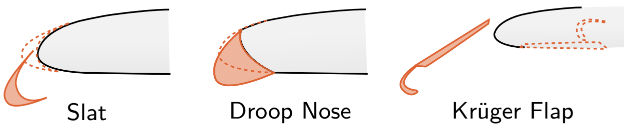

FIG 5. Considered device types

4.2. Actuator selection

Central to the actuation system is the selection of an actuator technology, which is first and foremost driven by the respective energy supply. Two main options for the actuators of the leading-edge system were initially identified: rotary electrically driven actuators and linear hydraulic actuators. A first comparison of electric and hydraulic actuators resulted in no feasible solution using electric actuators. The investigation shows that, generally, electric actuators are unable to be placed within the confined installation space between the leading edge and the front spar. Another drawback of using electrical actuation is the failure case of mechanical jams in the actuator. This is especially detrimental at the high rates required during load alleviation, as a sudden jam creates acceleration forces that can lead to structural deformation or damage. Aside from this, the investigated electric actuators caused a significant mass increase, likely negating the advantages of structural mass reduction enabled by the load alleviation capabilities. This can be explained by the low power density of electric actuators in comparison with their hydraulic counterparts. For hydraulic actuators, however, measures can be taken to minimise the inertia of the system and provide fast dynamics. This is crucial for the multifunctional leading-edge system, as the rates and accelerations necessary for effective load alleviation significantly surpass those of a conventional high-lift system. A primary measure to attain fast rates and reduce inertia is to prioritise a short stroke over the lower force generated by the actuator. This, however, means that the cylinder diameter must be increased, as the force results from the product of plunger area and hydraulic pressure. To counteract this effect, hydraulic pressure must be increased to avoid introduction of additional mass into the cylinder.

Equation 3 and Equation 4 are the equation of motion and pressure dynamics equation for the simplified hydraulic actuator displayed in Figure 6, where m is the mass of the actuator rod, p, A, and V describe the hydraulic pressure, plunger area, and volume in the respective chamber, $\sum F_{\mathrm{L}}$ are the load and friction forces acting against the direction of motion x, and Q_{in} and $Q_{\mathrm{L,i}}$ represent the incoming flow rate and internal leakage between the cylinder chambers of a hydraulic liquid with compressibility β.

(3) $$m \cdot \ddot{x} = p_{\mathrm{I}} \cdot A_{\mathrm{I}} - p_{\mathrm{II}} \cdot A_{\mathrm{II}} - \sum F_{\mathrm{L}}$$

(4) $$\dot{p}_{\mathrm{I}} = \frac{\beta}{V_{\mathrm{I}}} \left(Q_{\mathrm{in}} - A \cdot \dot{x} - Q_{\mathrm{L,i}} \right)$$

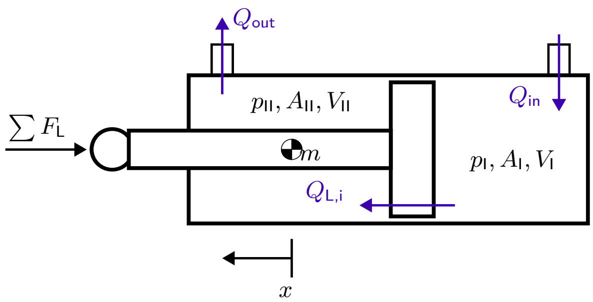

FIG 6. Schematic of a linear hydraulic actuator

From the equations above, it is evident that an increase in pressure not only allows a reduction of cylinder area, but also allows a reduction of flow rate, as cylinder area and volume are directly related. Furthermore, a short-stroke cylinder further aids in minimising the chamber volume. A low flow rate is also beneficial for the longevity of the system, as it helps to counteract or even fully avoid pressure drops that could cause cavitation in the hydraulic system. For these reasons, the implementation of the load alleviation function as part of the multifunctional system requires the use of hydraulic actuators, supplied by a high-pressure hydraulic system at a pressure level of 5000 psi.

4.3. System architecture

In addition to the selection of control devices and actuator technology, the system architecture and topology require further investigation in order to fulfil the previously defined system requirements. In terms of the actuation system, the challenge in the design of a multifunctional leading edge is the fusion of two different aircraft systems, namely a high-lift and a load alleviation system. There are stark differences between these two systems, as displayed in the simplified depiction in Figure 7. A conventional high-lift system is actuated from a central *power control unit* (PCU), which distributes rotational mechanical energy to the actuators of each control surface via a mechanical transmission shaft. Energy supply to the PCU may be either electric or hydraulic. Position sensors are installed at each end of the shaft in order to detect failure cases, e.g., a broken transmission shaft, through deviations in position at each shaft end. In case of failure, the system can be halted by a brake positioned at either end, which is integrated in the form of a wing-tip brake or as a power-off brake in the PCU. The common transmission shaft significantly simplifies failure monitoring and mitigation, as most relevant failure cases can be detected by monitoring the position and subsequently mitigated by arresting the entire system. In the case of a load alleviation system, a common mechanical transmission shaft cannot be used to power the droop noses. As discussed in section 3, each droop nose needs to be deployed to an individual position in order to effectively reduce the torsional moment on the wing. Therefore, the actuation of each of the outer droop noses must be independent. Nevertheless, with this solution, a high-lift operation, where all devices are deployed to the same position, remains plausible, which is required to fulfil high-lift requirements. For the inner droop nose devices, a central PCU is sufficient, as this control device is only used for high-lift operation. As this system is already proven, the following investigations are conducted with an emphasis on the outer droop nose devices used for load alleviation.

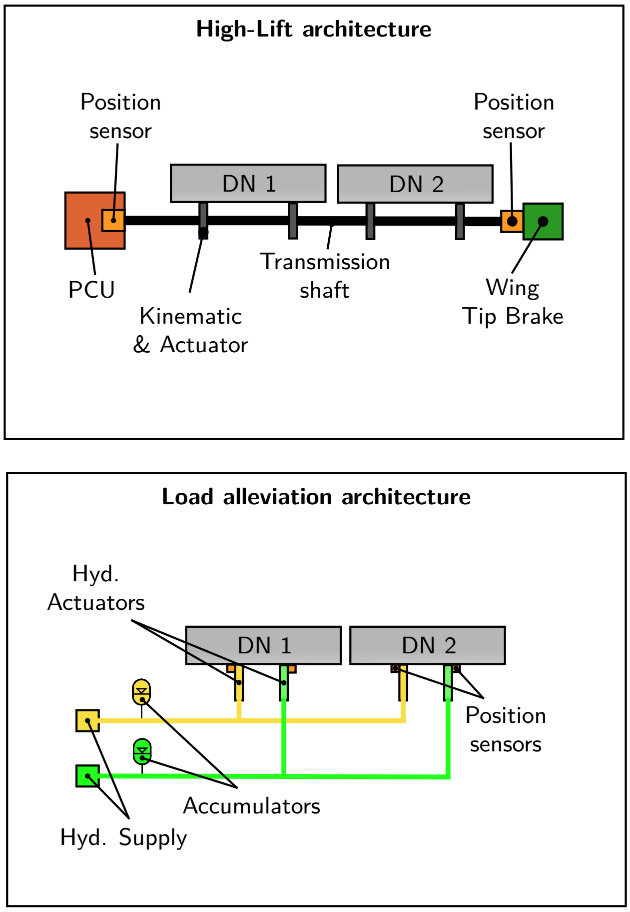

FIG 7. Comparison of high-lift and LAF system architectures

A second argument for an independent actuation system is the sizing of system components. In the case of a central drive, the drive would need to handle the sum of all droop nose loads. This would, as a result, require a large drive motor, producing greater system inertia and introducing significant additional system weight. For the multifunctional leading edge, there is no feasible solution using a central drive that could achieve the required actuation rates under the present load case. Implementation of a single-station drive, however, is detrimental to the monitoring concepts and the positional synchronization of the droop noses on the aircraft during high-lift operation. As the control devices are no longer connected by a common transmission shaft, a multitude of sensors must be implemented in the system architecture, since simple position monitoring using angular encoders at either end of the shaft is no longer effective. Secondly, a higher sensor bandwidth compared to high-lift system monitoring is required, as quicker actuator rates cause faster changes in system parameters. This also poses challenges to control computers, data buses, and the entire avionics system, since the multitude of data and signals must be processed and, if necessary, measures must be triggered without significantly increasing system reaction time due to delay. While the triggered measure for high-lift systems is the engagement of the brake, there is, as of yet, no detailed knowledge about the standard mitigation action for the multifunctional leading edge. In this work, ensuring a symmetric deflection of the control devices on both sides is assumed to represent a key target. However, it is not sensible to halt the entire system in the occurrence of any failure, as the system-level decoupling of the droop noses at the actuator level provides sufficient remaining system functionality. Nevertheless, a system-level solution for a safety device, comparable to the function of the safety brake in the high-lift architecture, must be provided. This must be implemented independently for every droop nose device, to be able to arrest droop noses individually in case of a runaway during operation. Additionally, it may be sensible to implement a solution for limiting the deflection of the droop noses for the use case of load alleviation in cruise. This measure should prevent the extension of the droop noses to the high-lift position under high loads. Considerations regarding a solution for such a safety measure shall be the topic of future work. Such a measure may not necessarily be a mechanical device but could also be implemented at the actuator or controller level.

From a system-technical point of view, the multifunctional leading edge is a high-lift system that is able to individually deploy the droop noses under cruise loads in a limited motion envelope. Therefore, the adaptation of monitoring and safety devices, which are already well established in high-lift architectures, is not only useful for the fast deflections of the load alleviation function but would also be required to demonstrate compliance with the certification requirements of high-lift systems. To establish a first idea of the achievable system safety of the multifunctional leading-edge system, preliminary system architectures are investigated. As previously discussed, the droop noses must be actuated by linear hydraulic actuators to attain the fast rates and high loads mentioned in section 3. Regarding the topology of the system architecture, two main variants of the system, each with its own benefits and drawbacks, are feasible. The main difference between these system architectures is the layout of the hydraulic power supply. One solution is the supply by central hydraulic circuits. In this variant, the hydraulic supply to the actuators requires at least two independent hydraulic circuits, since a single circuit would constitute a common failure source, leading to total loss of the system. It would nevertheless be highly desirable to design the system with only one actuator per droop nose, in order to avoid issues such as force fighting in an active-active configuration or losses caused by passively driving a second actuator. This solution, however, does not provide the minimum required failure probability of $F = 1 \cdot 10^{-5}$ per flight hour when considering a failure of four droop nose devices per wing as a total loss of the load alleviation function. Therefore, redundancy is provided both in the actuators, arranged in an active-passive configuration, and in the hydraulic power supply of the actuators. Furthermore, a hydraulic accumulator is placed near each actuator to mitigate pressure fluctuations. For system monitoring, position sensors are implemented at the actuators. The system is controlled by two independently running flight control computers, redundantly supplied by two electric networks.

The second variant is the actuation of the droop nose devices by electro-hydraulic actuators (EHAs). EHAs are actuators that include a local hydraulic circuit powered by an internal fixed-displacement pump, which is driven by an electric motor controlled by a motor control electronic (MCE). On the aircraft level, the system is supplied redundantly by the electrical network rather than a central hydraulic power supply. The main advantage of this solution in the context of the multifunctional leading edge is that each droop nose is actuated by a single EHA, so the failure of a hydraulic circuit no longer affects multiple droop nose devices. Furthermore, drawbacks associated with multiple actuators, e.g., force fighting in an active-active configuration or damping losses and “deadweight” of the passive actuator in an active-passive configuration, are eliminated. The rest of the system architecture is similar to the central hydraulic architecture discussed previously. In the EHA variant, the system is also monitored by a redundant sensor concept and controlled by two independent control computers. Both the hydraulic supply and accumulator are locally integrated into the EHA assembly. A simplified sketch of both architecture variants for one droop nose is displayed in Figure 8. For both system architecture variants, a reliability analysis was conducted. The reliability block diagram (RBD) for a single droop nose is provided in Figure 9, with the typical failure probability per flight hour given for each system component.

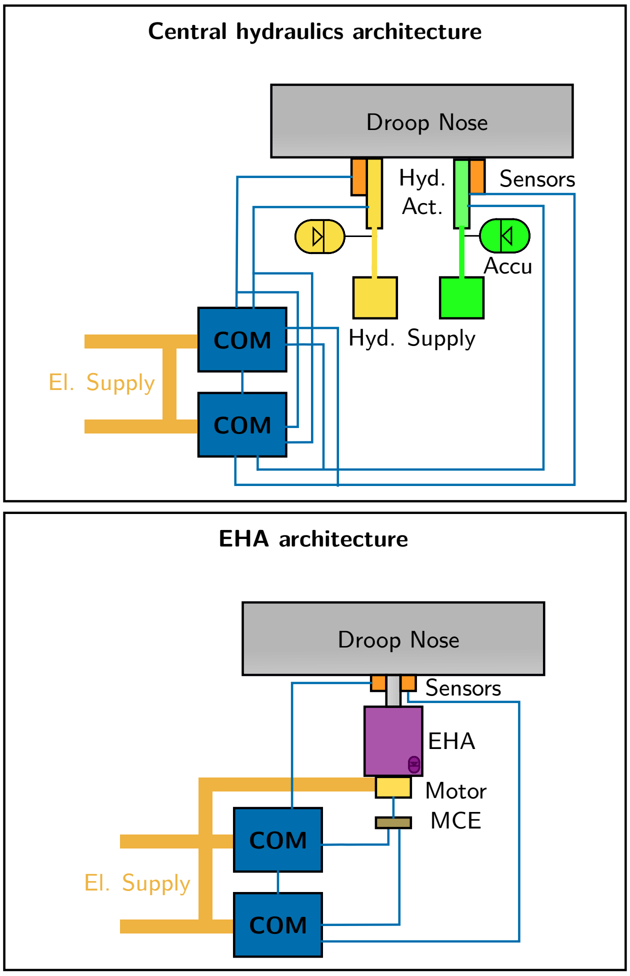

FIG 8. Sketch of system variants

The total failure probability for one of the droop noses in the central architecture results in $6.0 \cdot 10^{-9}$ per flight hour. The EHA architecture is significantly less reliable for a single droop nose, with the probability of failure for this variant summing up to $5.1 \cdot 10^{-5}$ per flight hour. However, all droop noses must be considered when calculating the total failure probability of the system. The failure of four devices results in a probability of $5.1 \cdot 10^{-9}$ occurrences per flight hour for the central hydraulic architecture and $2.51 \cdot 10^{-9}$ for the EHA architecture, respectively. Thus, the EHA architecture is more reliable regarding this failure case. On the aircraft level, there are a total of 140 different possible combinations in which four of the droop nose devices are in a failed state and thus lead to a total loss of the system function.

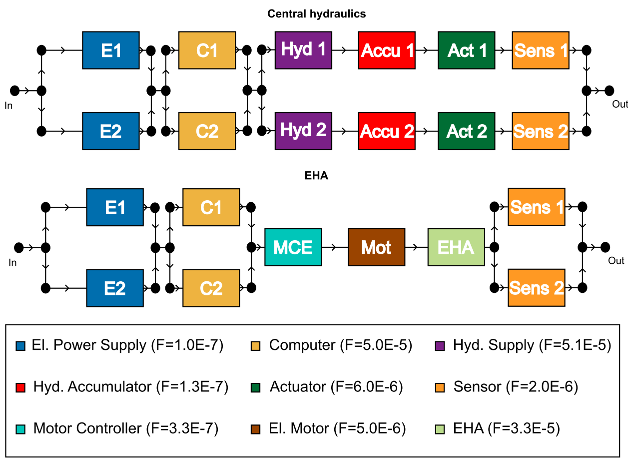

FIG 9. Reliability Block diagram of the system variants

The total probability of a system failure is therefore higher and equates to $7.2 \cdot 10^{-7}$ occurrences per flight hour for the central hydraulic architecture. In the case of the EHA, the total failure probability is $3.5 \cdot 10^{-7}$ occurrences per flight hour. Here, the EHA is also slightly advantageous compared to the central hydraulic architecture. Nevertheless, both values are well below the minimum requirement discussed in section 3. Therefore, both concepts of the system architecture are sufficient from a reliability viewpoint.

5. PRELIMINARY ACTUATOR SIZING

To estimate dimensions, system weight, and power consumption, a preliminary sizing of the hydraulic actuators is conducted using a tool developed at the Institute of Aircraft Systems Engineering of Hamburg University of Technology. The sizing investigation is based on the loads, control surface deflections and speeds, as well as the geometric constraints of the respective droop nose section. The relevant parameters of the actuator, e.g., mass, dimensions, stroke, and flow rate, are subsequently calculated according to the installation in the wing. A multitude of possible installations of the actuator in the wing is investigated during the process. A schematic of the sizing process is depicted in Figure 10.
Inputs to the sizing tool are the wing geometry as well as the system requirements, e.g., loads, droop nose deflection angles, and rates for all actuation system-relevant functions. The hinge point of every droop nose is fixed at the intersection of the wing profile and the front spar, and its deflection is modeled as a rotational movement about this hinge point.

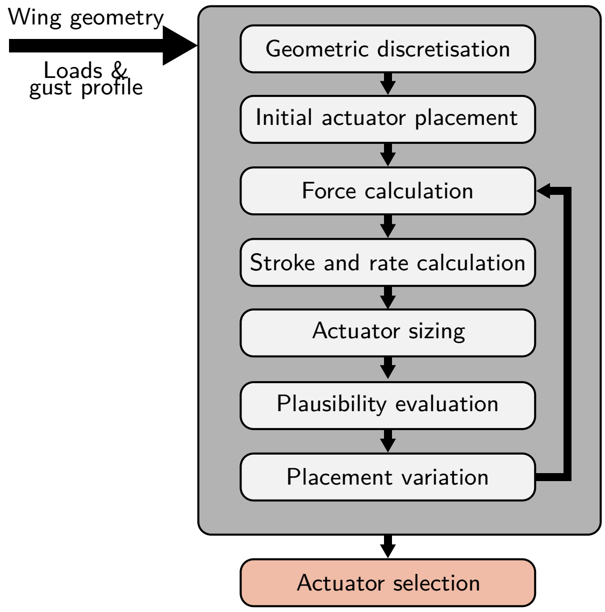

FIG 10. Schematic actuator sizing process

In a first step, the wing profile is reduced to the area of interest between the front spar and the profile nose. This section is subsequently discretised at a sufficiently small resolution. An initial placement of the actuator is chosen arbitrarily, from which the forces on the actuator can be calculated using the aerodynamic forces discussed in section 3. In addition to these, deformation forces caused by the structural deformation of the morphing droop noses are considered. The $1-\cos$ gust profile is used to establish the required rates and accelerations of the actuator during the critical gust encounter. The gust profile is also used to determine the piston stroke for every point in time during the gust encounter. However, the maximum stroke is dictated by the high-lift deflection of the droop noses. These parameters change depending on the placement of the actuator in the wing and impact the actuator dimensions as well as the hydraulic flow rate. Flow rate and power demand depend on the actuator dynamics. The actuator dimensions are determined from static parameters, e.g., the maximum deflection angles and the maximum forces acting in either direction. In addition to the maximum force, the plunger diameter is also sized according to the maximum stress in the actuator. The rod is hereby dimensioned to withstand buckling and strain forces. The plunger diameter must not be smaller than the diameter of the rod. The plunger diameter is subsequently used as the minimum inner diameter of the cylinder. A hoop stress calculation using thick-wall theory is performed in order to obtain the wall thickness and outer diameter of the cylinder. Using the dimensions of the actuator, the mass is calculated from the material volume of the actuator. Plausibility checking is subsequently conducted to exclude unrealistically large cylinders, cylinders that do not fit in the wing geometry or collide with it, as well as cylinders with an unrealistically low flow rate, mass, or stroke length. For each droop nose device, 20,000 actuators are investigated using a variation of the actuator rod fitting across 40 linearly distributed positions in the wing chord direction and 10 positions between the lower and upper surface of the wing. The actuator body fitting is varied across 5 different positions between the spar position and 2 % of the local chord length in front of the spar in chord direction, and 10 positions located between the upper and lower wing surface. For every droop nose section, multiple valid solutions are produced, ranging from 3 % of the total actuators of DN 9 to a maximum of

12 % of all actuators for DN 6. Out of these valid solutions, for every droop nose, two optimal actuators can be found: one with a minimum flow demand and one with minimal mass, as depicted in Figure 11.

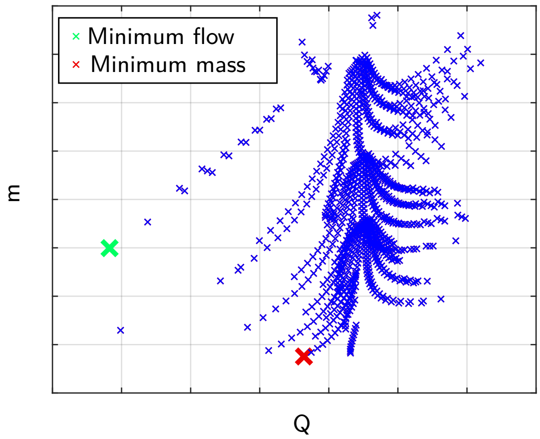

FIG 11. Optimal points for DN actuators

As mentioned previously, the parameters of the actuator solutions are dependent on the placement of the actuator in the droop nose. This applies to static parameters such as mass, as well as dynamic parameters such as flow and, in turn, power demand. This is caused by the line of action of the actuator force, which directly impacts how efficiently the actuator can generate a force to deflect its droop nose device. Based on this information, a heat map can be generated, highlighting the effect of attachment point variations. An exemplary heat map of the actuator mass in relation to the attachment point of the actuator rod is displayed in Figure 12.

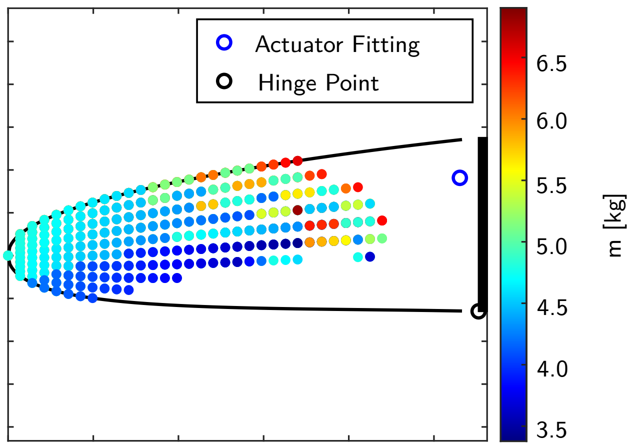

FIG 12. Actuator mass heat map

This heat map approach can be used for kinematic design, as the optimal points for actuator attachment are directly visible. This, in turn, is useful for identifying the next-best solutions if further restrictions prevent the design of the structural components from incorporating the exact attachment points at which an ideal solution is found.

5.1. Evaluation of sized actuators

As a first baseline for the actuators, the optimal point of the minimum flow rate for each droop nose actuator is chosen. In this consideration, it is assumed that the minimisation of power offers potential weight savings for the energy supply system of the actuator, since at low flow rates, lower power is demanded by the actuation system during operation, which in turn directly affects generators, supply cable cross sections, electrical motors, and hydraulic pumps of the EHAs, as well as the heat sink required for heat dissipation of the actuators. These factors are, as of yet, not considered within the sizing tool; therefore, the final result of the ideal-mass actuators is likely to diverge in the final system architecture. Nevertheless, a general trend of system weight and power demand can be identified using the preliminary design investigation. The actuator masses for all outer droop nose devices, as well as the power demands, are summarized in Table 3. The hydraulic power obtained from the actuators is converted to electrical power assuming a total motor and pump efficiency of $\eta_{\text{EHA}} = 0.8$ and a power factor of $PF = 0.6$.

	DN 2	DN 3	DN 4	DN 5	DN 6	DN 7	DN 8	DN 9
$m\,[kg]$	5.5	5.7	4.9	4.5	2.1	2.0	1.5	1.5
$P\,[kVA]$	6.7	15.4	11.8	10.2	6.5	5.0	3.8	3.1

TAB 3. Actuator masses and power demand

The total mass of the hydraulic cylinders equates to 25.7 kg per wing, or 51.4 kg for the overall aircraft. It is, however, important to notice that this weight only results from the cylinder itself and the actuator rods. The mass will therefore significantly increase when the additional components, such as hydraulic reservoirs, accumulators, pipes, and the electrical and mechanical components of the EHAs, e.g., motor pump, control electronics, and components such as heat sinks, are also considered in the future. Considering the results of KRALL [14], the system mass is likely to be double the amount of the preliminary architecture. In terms of power demand, the total amount of power required for the critical design case of load alleviation equates to 62.5 kVA per wing side, or 125 kVA in total. In section 3, a power budget of 310 kVA was attributed to the load alleviation function of the multifunctional leading edge system with additional load shedding. The result obtained from preliminary sizing shows that the required power falls significantly below this value. Therefore, it can be assumed that load shedding may, in fact, not be necessary for a discrete gust encounter. Nevertheless, means for attributing a higher load shedding could still be required when continuous turbulence is considered as a design case. If further budget is available, future approaches could consider a greater reduction in loads for the load alleviation system, provided that this offers promising benefits in terms of structural weight savings that can be obtained through future certification rules.

6. CONCLUSION

In the present paper, a novel leading edge system installed in a HLFC wing, providing multiple system functions such as high-lift capabilities and load alleviation functionality was proposed. Load alleviation technologies allow for a reduction of safety factor in structural mass design if a system failure probability lower than $1 \cdot 10^{-5}$ occurrences per flight hour can be mitigated. Especially, the bending moment reduction of trailing edge devices are promising for structural weight reduction and therefore enable higher aspect ratio wings. However, alleviation of bending moment causes an increase of the torsional moment on the wing root. This can be reduced by extending the load alleviation capabilities to the leading edge, which was previously utilised solely for lift augmentation. A reference aircraft to which a multifunctional leading edge system shall be applied was presented. It was shown that challenges arise for the design of an actuation system for the multifunc-

tional leading edge. These result from the critical load case of the reference aircraft, the integration of the system in the confined installation space of an HLFC wing and the power budgeting of the different aircraft functions as well as reliability and certification requirements for such a system. In order to use the benefits of laminar flow, a gap free control device in the form of a morphing droop nose must be used for a multifunctional leading edge system, as traditional control devices such as slats and Krüger flaps would cause a premature transition to turbulence. Based on the system requirements, two system architecture variants have been proposed, in which the inner droop nose device, which is only used for the lift augmentation function must be decoupled from the outer droop noses, which are deflected to independent deflection angles at independent deflection speeds. In both of these architecture variants, the outer droop noses are actuated by hydraulic actuators, since no viable solution using electromechanical actuation was found to the high rate requirements. System architecture solutions using conventional servo actuators as well as EHAs were discussed. Each of these variants has its own advantages and disadvantages, although both meet the minimum system safety requirements and are considered as a potential architecture solution. A preliminary sizing investigation of the droop nose actuators highlighted, that the placement of the actuator in the droop nose is a key factor to designing an actuation system which is capable of the combination of load alleviation an high-lift, while still comply with confined installation spaces and power budgets, without introducing unrealistically high system weight.
This work was primarily focused on highlighting the benefits of a multifunctional leading edge system and showing challenges that arise in the context of an actuation system design for the novel leading edge. While the additional investigation has shown, that a realisation of such an actuation system is theoretically possible, further investigation is necessary for in-depth system design. This includes the additional loads imposed by structural deformation and kinematics, additional mechanical, electrical and cooling components of the actuators as well as the influence of continuous gust encounters. Further investigation in this regard will produce more realistic results in terms of system topology, mass and reliability. Consideration of these factors will be necessary to evaluate the trade-off of the effort versus the benefits associated with the novel leading edge system.

ACKNOWLEDGEMENT

The results of the presented paper are part of the work in the research project *Multifunktionale Vorderkante für energieeffiziente Flugzeuge* (MUVE), which is supported by the Federal Ministry of Economic Affairs and Energy in the national LuFo VI.3 program. Funding code for TUHH: 20E2223C. Any opinions, findings and conclusions expressed in this document are those of the authors and do not necessarily reflect the views of the other project partners.

Supported by:

Federal Ministry
for Economic Affairs
and Energy

on the basis of a decision
by the German Bundestag

Contact address:

ole.krawehl@tuhh.de

References

[1] Fizaa Husain, Isabel Simmons, and David Zingg. *Application of Aerodynamic Shape Optimization to Swept Natural Laminar Flow Wings*. DOI: 10.2514/6.2024-3507.

[2] Michelle Lynde, Richard Campbell, Brett Hiller, and Lewis Owens. Design of a crossflow attenuated natural laminar flow flight test article. Technical report, NASA Langley Research Center, 01 2021. DOI: 10.2514/6.2021-0173.

[3] Michelle Banchy, Richard Campbell, and Brett Hiller. Crossflow attenuated natural laminar flow (catnlf) technology development: From concept to flight. Technical report, NASA Langley Research Center, 12 2022.

[4] Mark D Maughmer, Leonard P Metkowski, Christopher J Axten, and Dan M Somers. Application of a slotted, natural-laminar-flow airfoil to an 18-meter high-performance sailplane. In *AIAA SCITECH 2024 Forum*, page 0681, 2024.

[5] Michael S Selig, Mark D Maughmer, and Dan M Somers. Natural-laminar-flow airfoil for general-aviation applications. *Journal of aircraft*, 32(4):710–715, 1995.

[6] Max Kingsley-Jones. Farnborough: Aero secrets of boeing's new dreamliner. *Flight Global*, 18, 2014.

[7] Eric Miller. Approach for structurally clearing an adaptive compliant trailing edge flap for flight. 09 2015.

[8] Jia Xu and Ilan Kroo. Aircraft design with active load alleviation and natural laminar flow. *Journal of Aircraft*, 51(5):1532–1545, 2014.

[9] Andreas Hübner and Lars Reimer. Multidisciplinary simulation for gust load alleviation control surface analysis. In *Symposium der Deutsche Gesellschaft für Luft-und Raumfahrt*, pages 576–585. Springer, 2018.

[10] Lorenz Klug, Rolf Radespiel, Junaid Ullah, Ferdinand Seel, Thorsten Lutz, Jochen Wild, Ralf Heinrich, and Thomas Streit. *Actuator concepts for active gust alleviation on transport aircraft at transonic speeds*. DOI: 10.2514/6.2020-0271.

[11] Junaid Ullah, Thorsten Lutz, Lorenz Klug, Rolf Radespiel, and Jochen Wild. *Active Gust Load Alleviation by Combined Actuation of Trailing Edge and Leading Edge Flap at Transonic Speeds*. DOI: 10.2514/6.2021-1831.

[12] Junaid Ullah, Thorsten Lutz, Lorenz Klug, Rolf Radespiel, Jochen Wild, and Ralf Heinrich. Approach for aerodynamic gust load alleviation by means of spanwise-segmented flaps. *Journal of Aircraft*, 60(3):835–856, 2023. DOI: 10.2514/1.C037086.

[13] Marco Hillebrand, Christian Breitenstein, and Thorsten Lutz. Aeroelastic effects of a load alleviation system on a high aspect ratio wing based on cfd-csm simulations. 07 2024. DOI: 10.2514/6.2024-3841.

[14] Konstantin Krall, Lars-Hendrik Lemke, Frank Thielecke, J Müller, and C Breitenstein. *Systems for fast actuated droop noses and flap-tabs for dynamic load control*. Deutsche Gesellschaft für Luft-und Raumfahrt-Lilienthal-Oberth eV, 2024.

[15] Vasan Iyer and Oliver Bertram. Preliminary design and system considerations for an active hybrid laminar flow control system. *Aerospace*, 6:109, 10 2019. DOI: 10.3390/aerospace6100109.

[16] European Aviation Safety Agency. Certification Specifications and Acceptable Means of Compliance for Large Aeroplanes CS-25.

[17] Henning Strüber. The aerodynamic design of the a350 xwb-900 high lift system. In *29th international congress of the aeronautical sciences*. International Council of the Aeronautical Sciences, 2014.

[18] Greg A Whyatt and Lawrence A Chick. Electrical generation for more-electric aircraft using solid oxide fuel cells. Technical report, Pacific Northwest National Lab.(PNNL), Richland, WA (United States), 2012.

[19] Timo Pe and Frank Thielecke. Synthesis and topology study of hlfc system architectures in preliminary aircraft design. In *Proceedings of the 3rd CEAS Air&Space Conference, Venice, Italy*, pages 24–28, 2011.

[20] Konstantin Krall, Lutz Böhme, and Frank Thielecke. *Actuation systems for raised Krueger flaps on laminar airfoils*. Deutsche Gesellschaft für Luft-und Raumfahrt-Lilienthal-Oberth eV, 2024.

[21] Peter KC Rudolph. High-lift systems on commercial subsonic airliners. Technical report, 1996.

[22] Alessandro De Gaspari and Frédéric Moens. Aerodynamic shape design and validation of an advanced high-lift device for a regional aircraft with morphing droop nose. *International Journal of Aerospace Engineering*, 2019(1):7982168, 2019.